To cite this article: YANG Z K, ZHONG W B, FENG Y B, et al. Unmanned surface vehicle track control based on improved LOS and ADRC [J/OL]. Chinese Journal of Ship Research, 2020, 16(1). http://www.ship-research.com/EN/Y2020/V16/I1/121.

DOI: 10.19693/j.issn.1673-3185. 01842

Unmanned surface vehicle track control based on improved LOS and ADRC

YANG Zhongkai[1], *ZHONG Weibo*[*1,2], *FENG Youbing*[1], *SUN Bin*[1]

1 School of Electronics and Information, Jiangsu University of Science and Technology, Zhenjiang 212003, China

2 Marine Equipment and Technology Institute, Jiangsu University of Science and Technology, Zhenjiang 212003, China

Abstract: [**Objectives**] Under complex environmental conditions, unmanned surface vehicles (USVs) may deviate from the target course. In order to improve the anti-jamming ability and actual navigation stability and achieve accurate track control, this paper proposed an improved USV track control method. [**Methods**] According to the influence on navigation signals caused by the environment, track control is analyzed in two cases of GPS signal: effective and invalid. A track control method based on the line-of-sight (LOS) algorithm based on fuzzy-controlled variable ship-length ratios and the active disturbance rejection control (ADRC) algorithm is then realized on an autonomous controllable platform, and a lake test is carried out using a USV with dual propellers and dual rudders. [**Results**] The simulation results show that this method can meet the requirements of track control, and the heading can be stabilized quickly without frequent rudder swinging after turning. The proposed method can complete track control in real environments with an average track error of about 0.1 m and a variance of about 0.03. [**Conclusions**] The lake test results verify the feasibility and effectiveness of the proposed algorithm in practical engineering applications.

Key words: track control; LOS algorithm; ADRC algorithm; fuzzy control; autonomous controllable platform

CLC number: U664.82

0 Introduction

An unmanned surface vehicle (USV) is a kind of surface ship that can autonomously sail and complete its missions. It has a wide application prospect in military operations, maintenance of sea-area security, exploration of marine resources, and environmental monitoring [1]. The motion control of a USV mainly includes velocity and heading control, track control, intelligent planning, obstacle avoidance and navigation, and formation coordination. Specifically, track control is a premise for the USV to complete its mission independently, and also one of the core points for intelligent control of the USV [2-3].

The main methods for track control of a USV include line-of-sight (LOS) algorithms [4], backstepping sliding mode control [5], cascade PID [6], neural-network based control [7], robust adaptive control [8], and fuzzy control [9]. Tian et al. [10] designed and realized the tracking of straight lines by using LOS and anti-windup PID, solving the problem of heading overshooting and oscillation. However, in this method, heading accuracy and stability were greatly affected by external disturbances. Chen et al. [11] achieved a good tracking effect by combining an improved LOS algorithm with an adaptive sliding-mode heading-control algorithm and introducing an adaptive observer to estimate and compensate drift

Received: 2019 − 12 − 03 **Accepted:** 2020 − 02 − 05

Supported by: National Key R&D Program of China (2018YFC0309100); Key R&D Program of Jiangsu Province (BE2016009-3)

Authors: YANG Zhongkai, male, born in 1994, master degree candidate. Research interests: signal and information processing. E-mail: 649274721@qq.com

ZHONG Weibo, male, born in 1975, Ph.D., associate professor. Research interests: control theory and control engineering, communication and information systems. E-mail: vebo_cn@163.com

FENG Youbing, male, born in 1978, Ph.D., associate professor. Research interests: control theory and control engineering, communication and information systems. E-mail: 4450208@qq.com

***Corresponding author:** ZHONG Weibo

angles in real time. However, in the real-ship verification of the method, tracking errors of the USV were great at turning points of the desired track. On the basis of an LOS algorithm, Zhu et al. [12] analyzed the three control algorithms of incremental PID, fuzzy PID, and fuzzy PD with variable ship-length ratios through simulation. The results showed that fuzzy PD control with variable ship-length ratios was more advantageous in disturbance rejection. Fan et al. [13] designed a track-control algorithm combining LOS with fuzzy adaptive PID and tested the algorithm with a real ship. According to the results, the algorithm reduced the effects of time-varying drift angles on track control but resulted in a certain steering overshoot and a great position deviation at turning points of the path. Fossen et al. [14] combined a nonlinear adaptive integral LOS algorithm with a PID heading controller. According to their results, this method was suitable for the track control of a USV, but it took a long time for the USV to follow the desired path in the case of a change in path curvature.

Scholars have studied the theories, models, and realization methods for track control of a USV. However, the actual working environment of a USV is complex and changeable. In view of this, this paper studied the track control of a USV according to the effects of navigation signals and environment on the USV in actual navigation. A track-control method combining an LOS algorithm based on fuzzy-controlled variable ship-length ratios with an active disturbance rejection controller (ADRC) was proposed. First, a triangular track was simulated to verify the feasibility of this algorithm. Then, a lake test was carried out to verify the track-control effect of the USV.

1 Track-control method of USV

Due to environmental disturbances from winds, waves, currents, and shelters, a USV in actual navigation will deviate from its target course. In view of these problems, it is necessary to study the track control of a USV according to specific scenarios. In this paper, methods for track control were introduced in the case of effective and invalid GPS signals, respectively.

1.1 Track control in the case of effective GPS signals

The LOS algorithm is widely used in the track control of a surface ship. Essentially, it is to control the actual heading of a ship to align it with the LOS angle of the target heading, as shown in Fig. 1. In the figure, P_{k-1} is a track start point; P_k is a set target point; O is a real-time position of a USV. Let the longitudes and latitudes of points O, P_{k-1}, P_k, and P_{LOS}, be (O_{j}, O_{w}), ($P_{(k-1)\mathrm{j}}$, $P_{(k-1)\mathrm{w}}$), ($P_{k\mathrm{j}}$, $P_{k\mathrm{w}}$), and (P_{j}, P_{w}), respectively. A fan-shaped area is obtained by taking O as the center and an adjustable parameter R as the visual radius. Suppose that the USV has a length of L and a ship-length ratio of n. Then, there is $R=nL$ [12]. Δh is a track deviation. The fan-shaped area intersects the line $P_{k-1}P_k$ at P_{LOS}, and the direction of connection between O and the real-time target point P_{LOS} is the real-time target heading ψ_{r} with respect to true north. The actual heading ψ of the USV is obtained by GNSS, and the difference between ψ_{r} and ψ is the angle $\Delta\psi$ eliminating the track deviation. When the USV sails into the circular zone centered at P_k, it switches the target point to a new one. This process is repeated until the track control of the USV is finally completed.

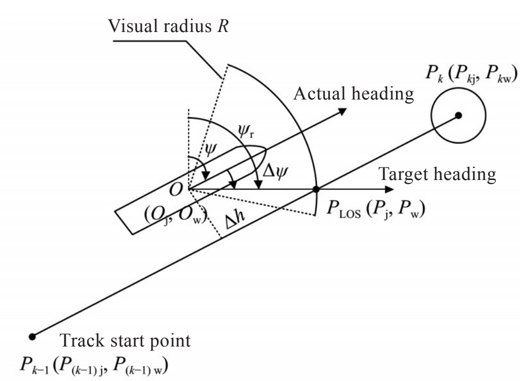

Fig. 1 Schematic diagram of LOS track control for USV

The coordinates of P_{LOS} can be obtained from Formula (1):

$$\begin{cases}(P_{\mathrm{j}}-O_{\mathrm{j}})^2+(P_{\mathrm{w}}-O_{\mathrm{w}})^2=R^2\\ \dfrac{P_{\mathrm{w}}-P_{(k-1)\mathrm{w}}}{P_{\mathrm{j}}-P_{(k-1)\mathrm{j}}}=\dfrac{P_{k\mathrm{w}}-P_{(k-1)\mathrm{w}}}{P_{k\mathrm{j}}-P_{(k-1)\mathrm{j}}}\end{cases} \tag{1}$$

The target heading can be obtained according to the longitudes and latitudes of points O and P_{LOS}.

$$\psi_{\mathrm{r}}=\arctan\left(\frac{(P_{\mathrm{j}}-O_{\mathrm{j}})\times\cos(O_{\mathrm{w}})}{P_{\mathrm{w}}-O_{\mathrm{w}}}\right) \tag{2}$$

1.2 Track control in the case of no GPS signals

In view of invalid GPS signals in the case of a USV passing through a bridge opening or a ship lock in actual navigation, this paper used an inertial-navigation fused processing method to ensure track control. As shown in Fig. 2, the USV passing through a bridge opening is taken as an example. It is assumed that GPS signals of the USV are invalid at point O. In such a case, the system needs to record the velocity v under the last effective GPS signal, the heading ψ_X from the inertial navigation equipment, and the distance d from the current position O of the USV to the target P_{k+1}. In order to reach the point P_{k+1}, the UAV sails with a target heading of $\psi_r = \psi_X$, a velocity of v, and duration of $t = d/v$. If GPS signals are still invalid after the duration of t, then the target heading ψ_{r+1} of the USV will be equal to the heading ψ_X provided by the inertial navigation equipment plus the heading deviation $\Delta\theta$ at the next point. $\Delta\theta$ is determined by Formula (4):

$$\psi_{r+1} = \psi_X + \Delta\theta \tag{3}$$

$$\Delta\theta = \psi_{k+2} - \psi_{k+1} \tag{4}$$

$$\psi_{k+1} = \arctan\left(\frac{(P_{(k+1)j} - P_{kj}) \times \cos(P_{kw})}{P_{(k+1)w} - P_{kw}}\right) \tag{5}$$

$$\psi_{k+2} = \arctan\left(\frac{(P_{(k+2)j} - P_{(k+1)j}) \times \cos(P_{(k+1)w})}{P_{(k+2)w} - P_{(k+1)w}}\right) \tag{6}$$

where ψ_{k+1} and ψ_{k+2} are the target heading of point P_{k+1} relative to point P_k and that of point P_{k+2} relative to point P_{k+1}, respectively, which are obtained by Formulas (5) and (6). With the repetition of the above process, track control of the USV in the case of invalid GPS signals can be realized.

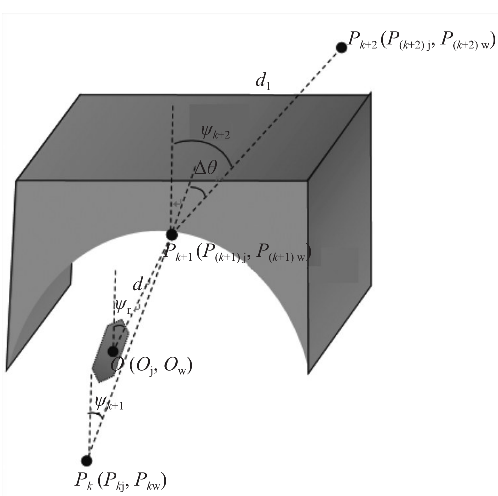

Fig. 2 Schematic of covered track control for USV

2 Track-control algorithm of USV

For the same target track, different visual radii R yield different effects of track control. In order to obtain the most suitable ship-length ratio n under the different environmental influences, we adopted fuzzy control to adjust n in real time. An ADRC was used for heading control. As fixed parameters are adopted in traditional PID control algorithms, it is difficult to select appropriate control parameters for these algorithms. With a transition process, the active-disturbance-rejection algorithm can compensate in real time and combine state errors nonlinearly. Fig. 3 shows the structural diagram of the track-control system, in which δ_r is an input to the control rudder and δ is a control variable acting on the USV model.

2.1 Fuzzy controller

For the fuzzy controller in Fig. 3, its inputs include a track deviation Δh and a track-deviation change rate dh from a real-time position to the target route, and its output is a variable ship-length ratio n. The system can adjust n in real time according to Δh and dh caused by environmental changes of the USV, so as to change R in the LOS algorithm to obtain the optimal target heading ψ_r.

2.1.1 Fuzzification and rule base

Considering the actual situation of the USV and accuracy of track control, quantitative domains of fuzzy variables of the fuzzy controller were designed as follows: track deviations E: [0, 4], track-deviation change rates EC: [−2, 2], and variable ship-length ratios N: [1, 4]. If the variables are out of the designed ranges, boundary values will be assigned. Specifically, track deviations are always positive and variable ship-length ratios N are of non-zero values. Fuzzy subsets corresponding to

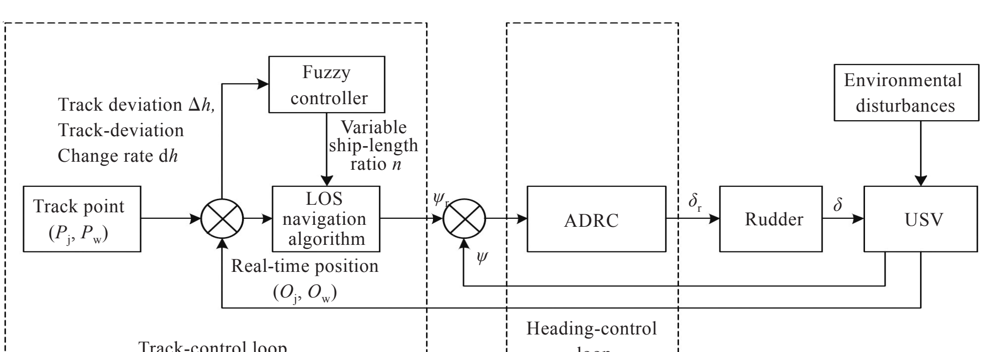

Fig. 3 System diagram of track control

various variables were as follows: $\widetilde{E}$={ZO, PVS,PS, PM,PB}, $\widetilde{EC}$={NB,NS,ZO,PS,PB}, $\widetilde{N}$={PVS, PS, PM, PB}. Normal Gaussian functions were adopted as membership functions of the fuzzy subsets. According to the experience of track control, the fuzzy rule table shown in Table 1 can be obtained.

Table 1 Fuzzy control table of ship-length ratios

EC	*E*				
	ZO	*PVS*	*PS*	*PM*	*PB*
NB	*PS*	*PS*	*PS*	PVS	*PVS*
NS	*PM*	*PM*	*PS*	*PVS*	*PVS*
ZO	*PB*	*PB*	*PS*	*PVS*	*PVS*
PS	*PM*	*PM*	*PS*	*PVS*	*PVS*
PB	*PS*	*PS*	*PS*	*PVS*	*PVS*

Functions of a variable ship-length ratio n are as follows: In the case of a small n, the USV can reach its target route more quickly under disturbances from winds, waves, and currents, but an overshoot can be easily caused. In the case of a large n, the USV can maintain its target heading smoothly, but it fails to approach its target route quickly due to disturbances from winds, waves, and currents. The main ideas of the fuzzy rule table in this paper are as follows: In the case of a large Δh, the USV deviates badly from the target route, and a small n should be used to make the USV approach the target route as soon as possible. In the case of a small Δh and a large dh, the USV is under environmental disturbances, and a small n should be used. In the case of a small Δh and a small dh, the USV is sailing stably, and a large n should be used. Thus, a USV in actual navigation can adapt to environmental changes quickly by adjusting n in real time through Δh and dh.

2.1.2 Defuzzification

As the fuzzy controller needs to output accurate values, defuzzification operations are necessary. Many defuzzification methods are available, and common ones include the weighted average method, the median method, and the area centroid method [15]. In this paper, the area centroid method was employed, with its specific formula as follows:

$$u=\frac{\sum_{k=1}^{m} u_k u_v(u_k)}{\sum_{k=1}^{m} u_v(u_k)} \tag{7}$$

where k is a variable; m is the number of elements in the fuzzy set; u_k is an element value of the fuzzy subset; $u_v(u_k)$ is the membership value of a corresponding element in the fuzzy subset; Σ refers to the summation of membership values of various elements in the output fuzzy subset; u is an output accurate value.

2.2 ADRC

The ADRC consists of three parts: a tracking differentiator, an extended state observer, and a feedback control law of nonlinear state errors. The tracking differentiator arranges a transition process and extracts a differential signal to solve an overshoot caused by an abrupt heading change. The extended state observer can not only observe headings but also estimate uncertain disturbances. The feedback control law of nonlinear state errors generates a control signal according to the nonlinear combination of errors between transition process and state estimations, as well as compensation for estimated disturbances [3]. Fig. 4 shows the structural diagram of the ADRC. In the figure, $V_0(k)$ is a target heading; $V_1(k)$ is a transition process of $V_0(k)$; $V_2(k)$ is the differential of the transition process; $e_1(k)$ and $e_2(k)$ are error functions of transition and observation signals; $U_0(k)$ is an intermediate control variable; $U(k)$ is an input rudder angle; $Y(k)$ is an actual heading; $Z_1(k)$−$Z_3(k)$ are observed states of the system; b_0 is a gain parameter.

The discrete expression of the tracking differentiator and the expression of the extended state observer used in the test of this paper are the same as those in Reference [16]. The PD control law of nonlinear state errors was used as the feedback control law of nonlinear state errors, as shown in Formula

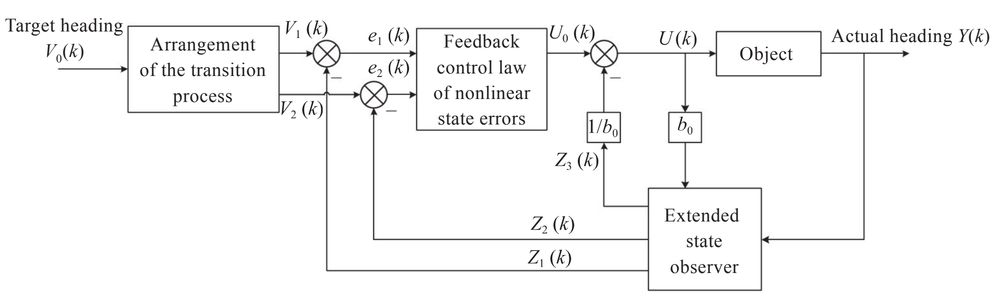

Fig. 4 Structure diagram of ADRC

(8). The nonlinear function fal in Formula (8) is the same as that in Reference [16]. k_p, k_d, δ_0, b_0 are adjustable parameters.

$$\begin{cases} e_1(k) = V_1(k) - Z_1(k) \\ e_2 = V_2(k) - Z_2(k) \\ U_0(k) = k_p \cdot fal(e_1, 0.65, \delta_0) + k_d \cdot fal(e_2, 1.5, \delta_0) \\ U(k) = U_0(k) - \dfrac{Z_3(k)}{b_0} \end{cases} \tag{8}$$

3 Design of control system and software

A domestic chip Loongson 1C and a domestic embedded real-time operating system RT-Thread were used as the autonomous controllable platform for USV control. The developed data acquisition and control board has various interfaces, with power supplies, sensors, control signals of motors and rudders, and communication modules all connecting to this board. Thus, time, velocity, azimuths, GPS states, longitudes and latitudes, attitudes, and distances from obstacles can be obtained through analysis by this board. In order to complete track control, we adopted a multi-thread design of RT-Thread. It mainly includes a sensor-data receiving and processing thread, a track-algorithm thread, a heading-control thread, a motor-rudder control thread, and an upper-computer data-interaction thread. Fig. 5 shows the flow chart of track control. First, the system receives data from each sensor and extracts effective ones through analysis. Then, it selects a track-control method according to GPS states and transmits the calculated pulse width modulation (PWM) value to a rudder. Finally, the rudder executes the command after receiving the signal.

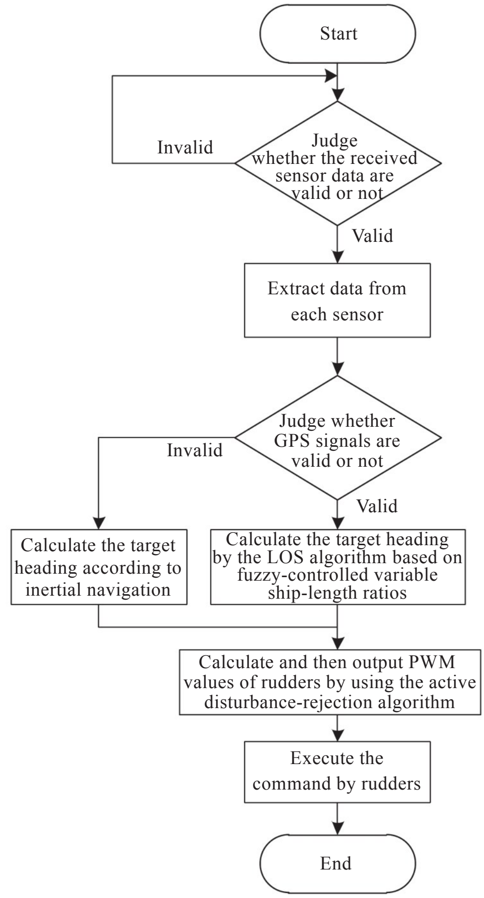

Fig. 5 Software block diagram of track control

4 Simulation of track control of USV

4.1 Simulation environment

According to the designed track-control algorithm, a simulation environment of track control was built through Simulink tools. Fig. 6 shows the block diagram of Simulink-based track control. This block diagram is mainly divided into three parts: a track-control loop, a heading-control loop, and a track-update loop.

The LOS algorithm based on fuzzy-controlled variable ship-length ratios was adopted for the track-control loop. Its inputs include the current position, the target position, and the visual radius calculated by the algorithm of fuzzy-controlled variable ship-length ratios, and its output is a target heading. An ADRC was used in the heading-control loop. The Nomoto model [17] expressed by Formula (9) was adopted as the mathematical motion model of the USV simulated in the heading-control loop. A first-order inertia model was employed as the rudder model, which is expressed by Formula (10). Disturbances of winds and waves to the navigation of a USV can be equivalent to those to rudder angles. White noise was applied to simulate disturbances from winds, waves, and currents, as expressed by Formula (11). In the track-update loop, the next position can be calculated according to the current position, velocity, and actual heading of the USV. Positions of the USV in the simulation algorithm are all represented by longitude and latitude coordinates.

$$G_1(S) = \frac{k_1}{(T_1 S + 1)S} \tag{9}$$

$$G_2(S) = \frac{1}{T_2 S + 1} \tag{10}$$

$$y(s) = h(s) \cdot \omega(s) = \frac{k_\omega s}{s^2 + 2\xi\omega_0 s + {\omega_0}^2} \cdot \omega(s) \tag{11}$$

where $G_1(S)$ is the transfer function of the Nomoto model; $G_2(S)$ is the transfer function of the rudder

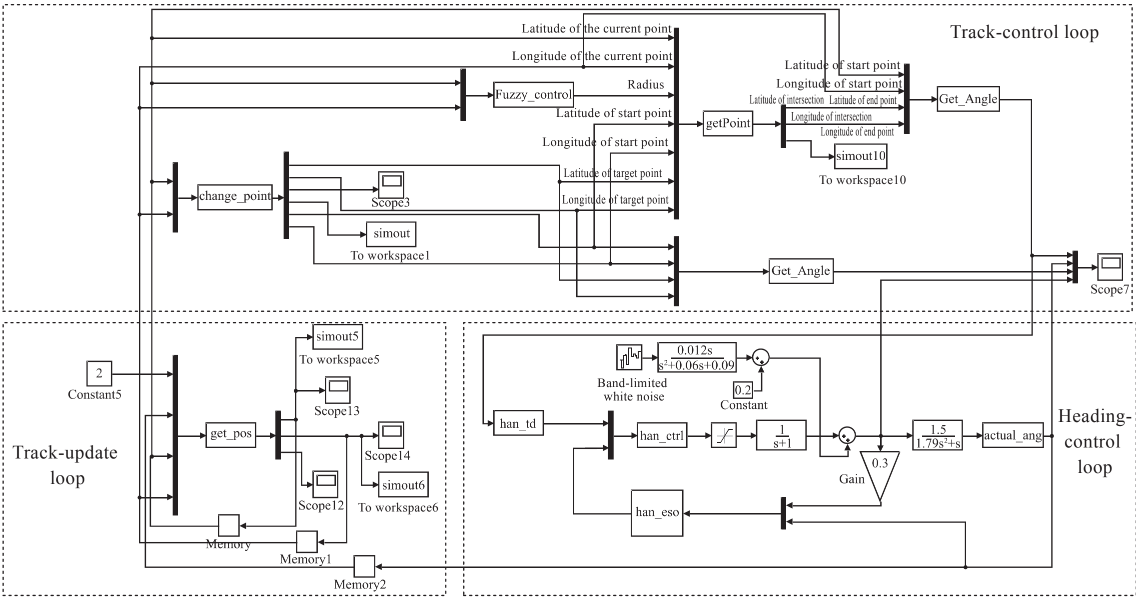

Fig. 6 System diagram of track control using Simulink

model; $y(s)$ is an equivalent rudder angle under wind-wave disturbances; $h(s)$ is the transfer function of a second-order wind-wave model; $\omega(s)$ is an input of the disturbance model, which is Gaussian white noise with a mean of 0 and power spectral density of 0.1; k_1 is a maneuverability index; $k_\omega = 2\xi\omega_0\sigma$, where ξ, ω_0, and σ are the damping coefficient, wind-wave frequency, and wind-wave intensity, respectively.

4.2 Experimental simulation

A triangular track was simulated. In the simulation, parameters of Formula (8) were set as follows: k_p =0.9, k_d = 1.2, δ_0 = 0.02, and b_0 = 0.3; parameters of Formula (11) were set as follows: ξ=0.1, ω_0 = 0.3, and σ = 0.2; velocity was set to 2 m/s. The longitudes and latitudes of the three target points in the simulation were as follows: A (119.460 934 101 7°, 32.198 867 838 3°), B (119.461 125 181 7°, 32.198 695 635 0°), and C (119.460 876 234 6°, 32.198 674 479 7°). With point A as the start point and due north as the initial heading, track simulation was done from point A to point B and then to point C. Fig. 7 shows the simulated track of the USV.

From Fig. 7, the USV can sail along the set track with natural transitions at turning positions. Turning with obtuse angles can better prove the fast adaptability of the algorithm. As can be seen from the figure, the USV makes a large turn near the target point. At this time, both the track deviation and its change rate are large. In view of this, the fuzzy controller will output an appropriate ship-length ratio according to the fuzzy rules. Thus, a target heading

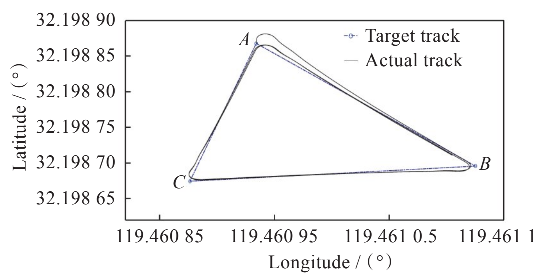

Fig. 7 Diagram of track

for approaching the desired route faster can be obtained, making the actual route close to the target one quickly, with no large overshoot.

Fig. 8 shows the simulated headings and rudder angles of the USV. With the due north as the initial heading, the USV reaches the target heading within 5 s. Then, it keeps the heading stable, with a smooth heading curve, under environmental disturbances. After turning, it can reach the target heading quickly, with basically no overshoot. The actual heading of the USV is between 0° and 360°. When the target heading of the USV changes from 264° to 16° at 90 s, the USV first increases the angle from 264° to 360°, and then from 0° to 16°. This meets the requirement of the actual navigation of the USV. In Fig. 8, the rudder angle of 0° indicates the middle position at the beginning. A rudder angle greater than 0° indicates rightward steering, while a rudder angle less than 0° indicates leftward steering. In the case of target-point switching, a large rudder angle is first needed, and when the target heading is reached, the rudder angle gradually tends to 0°. This proves the effectiveness of the ADRC in this paper.

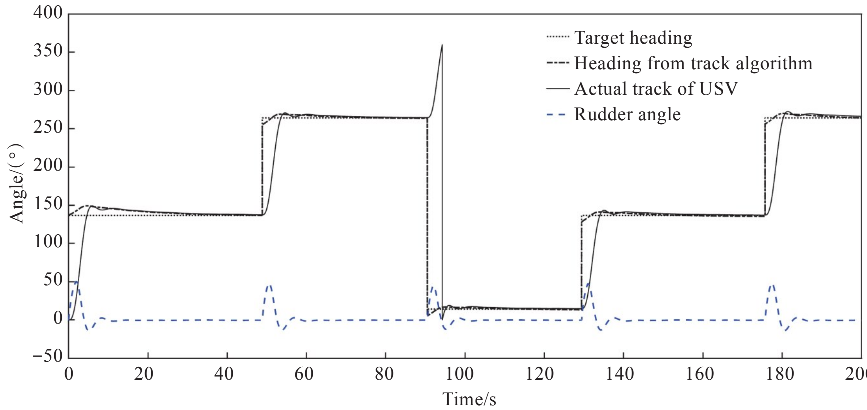

Fig. 8 Simulation result of headings and rudder angle of USV

5 Test results and analysis

A dual-propeller dual-rudder USV was tested, with a length of 1.4 m and a width of 0.35 m. The external high-precision differential GPS had a positioning accuracy up to 10 cm. The integrated inertial-navigation system could output headings with angular errors up to 0.5° after the filtering fusion algorithm. Two groups of customized lithium batteries were used. When each group has a capacity of 13 600 mA, the maximum load current is 80 A. The test was conducted in Wanpingkou Lagoon in Rizhao, Shandong Province, at temperature of 18 ℃ and northeast wind of scale 4. The route had a total length of 5 km, and the USV was required to pass through four bridge openings. Specifically, the narrowest bridge opening had a width of about 3 m. Fig. 9 shows the test USV. During the autonomous navigation, data and videos of the USV were uploaded in real time, and displayed in the user interface, as shown in Fig. 10.

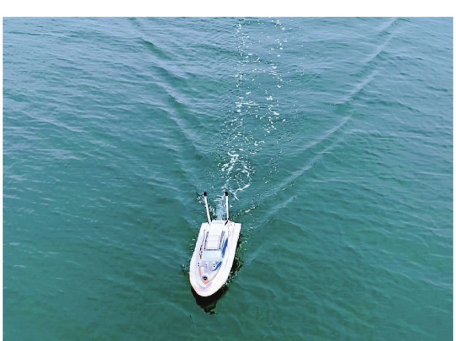

Fig. 9 Tested USV

GPS data during the navigation of the USV were recorded. Target and actual routes in the 5 km navigation of the USV were compared in the coordinate system with longitudes as abscissas and latitudes as ordinates. In the test, there were 92 target route points and 5 000 actual GPS points. Four bridge

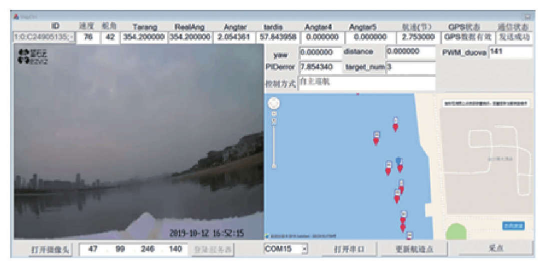

Fig. 10 User interface

openings were passed through during the navigation, as shown in Fig. 11.

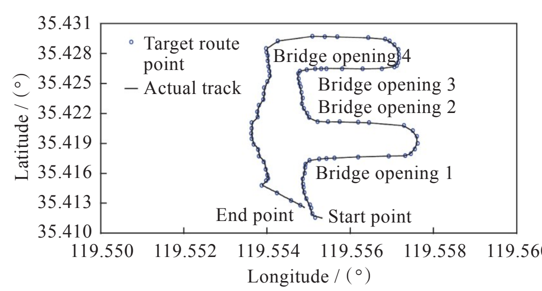

Fig. 11 Track tracing results

According to Fig. 11, the USV can autonomously navigate according to the set target route, and pass through the bridge openings without GPS signals. In order to verify the tracking accuracy, this paper calculated the track deviations of track points of 5 km, as shown in Fig. 12. From the figure, the average track error is about 0.1 m, and the variance is about 0.03. The maximum track deviation is about 1.5 m, at a time of track-point switching. However, with the LOS algorithm based on fuzzy-controlled variable ship-length ratios, as well as the ADRC, the USV can quickly reduce the track deviation to less than 1 m. In Reference [13], the USV "Haixun 03" had a maximum error of about 20 m during its navigation between Qingdao and Lianyungang. By comparison, the USV track-control algorithm based on the autonomous controllable platform proposed in this paper has high control precision and can make real-time adjustments according to environmental conditions. Thus, it can meet the requirement of the actual navigation of a USV.

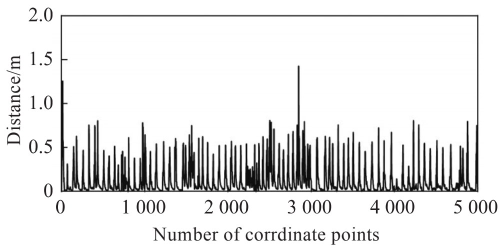

Fig. 12 Track error of USV

6 Conclusions

Considering environmental disturbances to USVs in navigation, with regard to tracking control of USVs in the real environment, this paper designed and realized a track-control method combining the LOS algorithm based on fuzzy-controlled variable ship-length ratios with an ADRC. Moreover, a simulation test with a triangular track was conducted. From the simulation results, this algorithm can realize the track control of the desired path. It can quickly restore the track after a large turning to the desired one, with a stable heading and no large overshoot. This verifies the stability and reliability of the algorithm.

The control strategy and algorithm given in this paper were realized based on the autonomous controllable platform and verified through actual navigation of a dual-propeller dual-rudder USV. From the test results, the strategy and method proposed in this paper can well control the track of the USV in the real environment, with an average track error of about 0.1 m and a variance of about 0.03.

References

[1] LIU C G, CHU X M, WU Q, et al. A review and prospect of USV research [J]. Shipbuilding of China, 2014, 55 (4): 194−205 (in Chinese).

[2] LIAO Y L, ZHANG M J, DONG Z P, et al. Methods of motion control for unmanned surface vehicle: state of the art and perspective [J]. Shipbuilding of China, 2014, 55 (4): 206−216 (in Chinese).

[3] WANG C S, XIAO H R. Path following controller for unmanned surface vessels based on ADRC [J]. Journal of Shandong University (Engineering Science), 2016, 46 (4): 54−59, 75 (in Chinese).

[4] BORHAUG E, PAVLOV A, PETTERSEN K Y. Integral LOS control for path following of underactuated marine surface vessels in the presence of constant ocean currents [C]//Proceedings of the 2008 47th IEEE Conference on Decision and Control. Cancun: IEEE, 2008: 4984−4991.

[5] YU Y L, SU R B, FENG X, et al. Tracking control of backstepping adaptive path of unmanned surface vessels based on surge-varying LOS [J]. Chinese Journal of Ship Research, 2019, 14 (3): 163−171 (in Chinese).

[6] ZHONG W B, LU Z C, FENG Y B, et al. Design and implementation of motion control system for unmanned surface vessel with two propellers [J]. Shipbuilding of China, 2019, 60 (3): 194−202 (in Chinese).

[7] DONG Z P, LIU T, WAN L, et al. Straight-path tracking control of underactuated USV based on Takagi-Sugeno fuzzy neural network [J]. Chinese Journal of Scientific Instrument, 2015, 36 (4): 863−870 (in Chinese).

[8] DO K D. Global robust adaptive path-tracking control of underactuated ships under stochastic disturbances [J]. Ocean Engineering, 2016, 111: 267−278.

[9] ZHONG W B, LUO Y, LU D H, et al. Design and implementation of communication navigation and control system for unmanned surface vehicle [J]. Shipbuilding of China, 2018, 59 (1): 207−215 (in Chinese).

[10] TIAN Y, WANG D, PENG Z H, et al. Design and validation of path tracking controller for USV along straight-lines [J]. Journal of Dalian Maritime University,2015, 41 (4): 14−18 (in Chinese).

[11] CHEN X, LIU Z, LUO Y S, et al. Path tracking control algorithm for the underactuated USV in the marine environment [J]. Journal of Harbin Institute of Technology, 2018, 50 (10): 110−117 (in Chinese).

[12] ZHU J, WANG J H, ZHAO M K, et al. Simulation of path following optimization control of unmanned surface vehicle [J]. Computer Simulation, 2016, 33 (6): 362−367 (in Chinese).

[13] FAN Y S, GUO C, ZHAO Y S, et al. Design and verification of straight line path following controller for USV with time-varying drift angle [J]. Chinese Journal of Scientific Instrument, 2016, 37 (11): 2514−2520 (in Chinese).

[14] FOSSEN T I, PETTERSEN K Y, GALEAZZI R. Lineof-sight path following for dubins paths with adaptive sideslip compensation of drift forces [J]. IEEE Transactions on Control Systems Technology, 2015, 23 (2): 820−827.

[15] LIN Z, LYU X F. Autonomous obstacle avoidance of unmanned surface vessel based on improved fuzzy algorithm [J]. Journal of Computer Applications, 2019, 39 (9): 2523−2528 (in Chinese).

[16] HAN J Q. Auto disturbances rejection control technique [J]. Frontier Science, 2007 (1): 24−31 (in Chinese).

[17] JIA X L, YANG Y S. Mathematical model of ship motion: mechanism modeling and identification modeling [M]. Dalian: Dalian Maritime University Press, 1999 (in Chinese).

基于改进的视线导引算法与自抗扰航向控制器的无人艇航迹控制

杨忠凯[1], 仲伟波[*1,2], 冯友兵[1], 孙彬[1]
1 江苏科技大学 电子信息学院,江苏 镇江 212003
2 江苏科技大学 海洋装备研究院,江苏 镇江 212003

摘 要: [目的] 无人艇(USV)在复杂环境情况下会出现偏离目标航线的情况,为提高水面无人艇的抗干扰能力及实际航行的稳定性,实现对航迹的准确控制,提出一种改进的无人艇航迹控制方法。[方法] 根据导航信号受环境影响的情况,对GPS信号有效和无效2种情况下的航迹控制分别进行分析,在自主可控平台上设计并实现了基于模糊控制可变船长比的视线导引算法(LOS)和自抗扰航向控制器(ADRC)相结合的航迹控制方法,并开展了双桨双舵无人艇湖上试验。[结果] 仿真结果表明:该方法可满足航迹控制的要求,转弯后航向能够快速保持稳定,无频繁摆舵现象,且该方法能够完成真实环境下的航迹控制,航迹贴线误差均值约为0.1 m,方差约为0.03。[结论] 湖上试验结果验证了该算法在实际工程应用中的可行性和有效性。

关键词: 航迹控制; 视线导引算法; 自抗扰算法; 模糊控制; 自主可控平台

[*Continued from page* 51]

[16] YASUKAWA H, YOSHIMURA Y. Introduction of MMG standard method for ship maneuvering predictions [J]. Journal of Marine Science and Technology, 2015, 20 (1): 37–52.

[17] LIU J L, QUADVLIEG F, HEKKENBERG R. Impacts of the rudder profile on manoeuvring performance of ships [J]. Ocean Engineering, 2016, 124: 226−240.

[18] WANG Y. Modeling and path tracking control of unmanned surface vessel [D]. Hangzhou: Zhejiang University, 2019 (in Chinese).

[19] ZHONG H X, QIU S H, LUO X SH, et al. Study of applying BP neural network with inertia term self-tuning to attitude stability of quadrotor unmanned aerial vehicle [J]. Journal of Guangxi Normal University (Natural Science Edition), 2017, 35 (2): 24−31 (in Chinese).

基于深度强化学习的智能船舶航迹跟踪控制

祝亢[1], 黄珍[*1], 王绪明[2]
1 武汉理工大学 自动化学院,湖北 武汉 430070
2 武汉理工大学 智能交通系统研究中心,湖北 武汉 430063

摘 要: [目的] 智能船舶的航迹跟踪控制问题往往面临着控制环境复杂、控制器稳定性不高以及大量的算法计算等问题。为实现对航迹跟踪的精准控制,提出一种引入深度强化学习技术的航向控制器。[方法] 首先,结合视线(LOS)算法制导,以船舶的操纵特性和控制要求为基础,将航迹跟踪问题建模成马尔可夫决策过程,设计其状态空间、动作空间、奖励函数;然后,使用深度确定性策略梯度(DDPG)算法作为控制器的实现,采用离线学习方法对控制器进行训练;最后,将训练完成的控制器与BP-PID控制器进行对比研究,分析控制效果。[结果] 仿真结果表明,设计的深度强化学习控制器可以从训练学习过程中快速收敛达到控制要求,训练后的网络与BP-PID控制器相比跟踪迅速,具有偏航误差小、舵角变化频率小等优点。[结论] 研究成果可为智能船舶航迹跟踪控制提供参考。

关键词: 智能船舶; 航迹跟踪控制; 深度强化学习; 视线导航法